Inorganic Chemistry
Cite This: Inorg. Chem. 2019, 58, 3627−3634
Article
pubs.acs.org/IC

Overlap of Radial Dangling Orbitals Controls the Relative Stabilities of Polyhedral B_nH_{n-x} Isomers (n = 5−12, x = 0 to n − 1)

Naiwrit Karmodak, Rinkumoni Chaliha, and Eluvathingal D. Jemmis*

Inorganic and Physical Chemistry Dept., Indian Institute of Science, Bangalore 560012, Karnataka, India

Supporting Information

ABSTRACT: The removal of H atoms from polyhedral boranes results in the formation of dangling radial orbitals with one electron each. If there is a requirement of electrons for skeletal bonding to meet the Wade's rule, these are provided from the exohedral orbitals. Additional electrons occupy a linear combination of the dangling orbitals. Stabilization of these molecular orbitals depends on their overlap. The lateral (sideways) overlap of dangling orbitals decreases with the decreasing cluster size from 12 to 5 boron atoms as the orbitals become more and more splayed out. Thus, as the number of dangling orbitals increases, the destabilization of their combinations increases at a higher rate for smaller polyhedral boranes, leading to flat structures with the removal of a fewer number of hydrogens. Though exohedral orbitals form better overlap in larger polyhedral clusters, the increase of electrons with the removal of H atoms results in occupancy of antibonding skeletal orbitals (beyond Wade's rules) and leads to flat structures. The reverse happens when hydrogens are added to a flat cluster. Substitution of BH by Si does not change structural patterns.

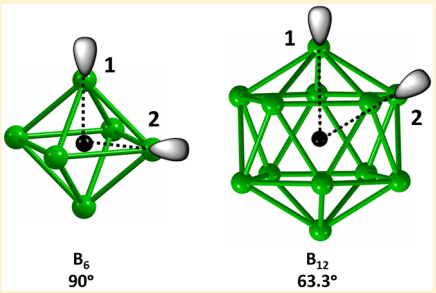

INTRODUCTION

The ubiquitous icosahedral B_{12} and other polyhedral structures dominate elemental boron and its molecular structures.[1−5] Though computational studies by Boustani and others proposed planar structures for pure boron clusters over 20 years ago,[6−10] only in recent years experimental methods designed by Wang and co-workers brought them into existence.[11−16] Adaptive Natural Density Partitioning technique (AdNDP) by Boldyrev and co-workers provided a way to describe bonding in these novel clusters.[17,18] Among several experimental attempts, mass spectrometric analysis of $B_{12}H_x^+$ clusters produced in an ion trap chamber gave a head start in conjunction with theoretical structural search.[19,20] It showed that the transformation of the icosahedral borane to a flat structure takes place when the number of hydrogens is decreased; the tipping point is estimated at x = 4.[19] A majority of the clusters obtained have seven and eight H atoms. $B_{12}I_{12}^{2-}$ also shows structural transformations, when iodine atoms are detached consecutively.[21,22] On the other hand, planar boron-only clusters transform to cage geometries on the addition of H atoms.[23−25] Wang and co-workers generated a series of $B_nD_2^-$ molecules in the gas phase with n varying from 7 to 12. Elongated planar double chain (DC) structures are characterized for these clusters, using experimental photoelectron spectra and theoretical calculations.[26−28] The doping of the planar boron clusters with the heteroatoms is also found to have severe structural deformations.[29−35]

The structural transformations brought by varying the electron count are common in chemistry. Addition of electrons often makes the structure flat, whereas depletion of electrons forces the atoms to cluster into cages to share available electrons, as seen in going from C_6H_6 (D_{6h}) to $C_6H_6^{2+}$ (C_{5v}) to $B_6H_6^{2-}$ (O_h, the equivalent of $C_6H_6^{4+}$).[36−40] The variation in the electrons has been shown to modulate the stability and structure of boron clusters.[41] However, the orientation and overlap of adjacent radial π orbitals must also contribute to the structural preferences of the boron clusters. When the radial orbitals overlap strongly, the resulting delocalized stable molecular orbitals will be able to accommodate electrons easily; these will not be pushed to the antibonding skeletal orbitals.

The overlap for the radial orbitals in small polyhedral clusters is not substantial due to the splaying out of these orbitals as shown in Figure 1. A comparison of the splaying nature of radial orbitals for the four cage boron clusters, such as B_6, B_{12}, B_{20}, and B_{40}, is depicted by subtending the angle between two adjacent boron atoms on the surface of the cage to the centroid (black sphere, Figure 1). The angle decreases substantially from B_6 to B_{40} and the radial overlap would become better.[10,12,16,42] Thus, the cage geometries for B_nH_x with appropriate electron counts become more favorable as the size of the cluster increases. The diffuseness of the radial p orbitals also varies by doping with the heteroatoms. A similar possibility exists for flat structures as well.[43] The effect of overlap of radial dangling orbitals formed after removal of H atoms from polyhedral boranes in shaping the cluster geometries is quantitatively studied in this article for polyhedral B_nH_x clusters, by varying the sizes from 5 to 12 and $x \leq n$. The topology of the polyhedron decides the angular

Received: October 21, 2018
Published: February 27, 2019

DOI: 10.1021/acs.inorgchem.8b02986
Inorg. Chem. 2019, 58, 3627−3634

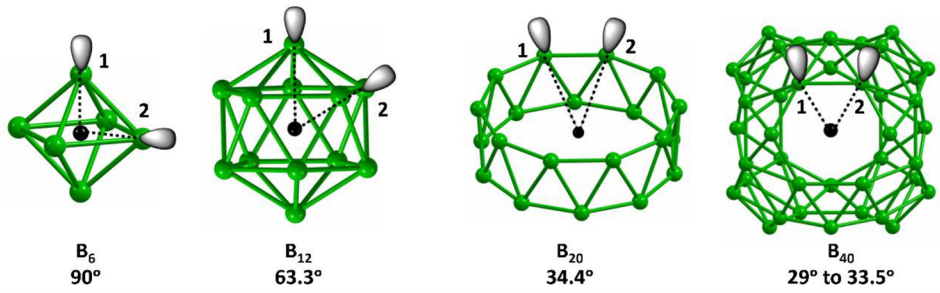

Figure 1. The angle (in degrees) subtended by two adjacent boron atoms on the surface denoted as 1 and 2 to the centroid shown in black sphere.

direction of the dangling radial orbitals and therefore must determine the structural transition points from 3D to 2D geometries upon removal of H atoms. The corresponding Si-doped boron clusters, being isolobal to the BH units, have also been studied by varying the cluster sizes. The spatial topology and the overlap of these radial dangling orbitals are found to be essential in satisfying the skeletal electron counts of polyhedral B_nH_x clusters and tipping the structural transition points.

COMPUTATIONAL DETAILS

The computations are performed with the Density Functional method using the Gaussian 09 package.[44] Both restricted and unrestricted calculations are performed for the clusters with the even number of electrons, whereas only unrestricted calculations are performed for those clusters having an odd number of electrons. The meta-hybrid functional, TPSSh, is used to incorporate the Coulomb and exchange correlations.[45−47] The basis set functions for the atomic orbitals are denoted by the triple-ζ (split-basis) basis set, 6-311+G(d,p).[48−50] In a recent benchmark study, it has been shown that relative energy of the planar vs caged isomers is better represented at the TPSSh level.[41,51] The frequencies are calculated to confirm the stability of the structures on the potential energy surface. In case negative frequencies are obtained, the structures are distorted to follow the frequencies along the potential energy surface in order to obtain minima. The energy corrections for most stable isomers of $B_{12}H_x$ clusters obtained at TPSSh/6-311+G(d,p) are done by performing a single point energy calculation at CCSD/6-311+G(d,p) and CCSD(T)/6-311+G(d,p).[52−54] The relative stability trend at both CCSD and CCSD(T) shows slight variations (within the range of 5 kcal/mol) for $B_{12}H_x$ clusters only at x = 3 and 5 (Table T1, Supporting Information); hence, for other B_nH_x clusters, the energy correction is done only at CCSD/6-311+G(d,p). In order to check the accuracy of the methods used in this study, we have calculated the relative stability of $B_{12}H_x$ clusters by optimizing at CCSD(T)/def2TZVP//B3LYP-D3/def-2TZVP. The relative stability of these isomers is found to remain unchanged as shown in Table T1 (Supporting Information). The orbital interaction diagram is plotted using the Amsterdam Density Functional (ADF) package[55] at TPSSh functional and Triple Zeta with polarization basis set.

RESULTS AND DISCUSSION

Let us begin with $B_{12}H_{12}^{2-}$, which obeys the Wade's rules. If we remove a H atom from $B_{12}H_{12}^{2-}$ by breaking a B−H bond, the unpaired electron in the resulting $B_{12}H_{11}^{2-}$ radical is in a dangling high energy orbital (Figure 2a). This is not a favorable situation. However, if the same exercise is carried out on $B_{12}H_{12}^{-}$ radical (one unpaired electron), which requires an additional electron to attain the Wade's rule, a stabilizing situation emerges. $B_{12}H_{11}^{-}$, obtained by removing a H atom, has now an option to place the electron from the dangling high energy orbital to the skeletal bonding MOs, thus satisfying the Wade's rule (Figure 2b). Let us do this exercise with neutral $B_{12}H_{12}$, which requires two electrons more for satisfying the

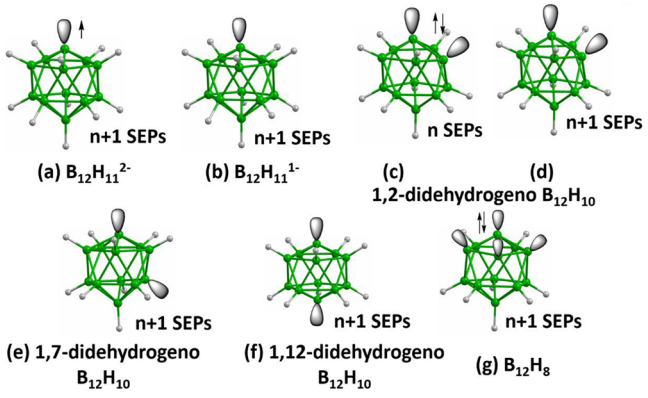

Figure 2. Schematic diagram showing the electron counting rules for $B_{12}H_x$ clusters. SEPs denote the skeletal electron pairs. (a) $B_{12}H_{11}^{2-}$ with one unpaired electron in the dangling radial orbital. (b) $B_{12}H_{11}^{-}$ which satisfies the Wades rules (n+1 SEPs). (c) $B_{12}H_{10}$ with only n SEPs and the filled splayed out π MO. (d−f) n+1 SEPs requirement met, vacating the dangling orbitals. (e, f) More stable than (d) from better hyperconjugative stabilization. (g) Most stable isomer of $B_{12}H_8$ where the two excess electrons, after satisfying the SEPs, occupy the bonding combination of dangling orbitals.

Wade's rule. The removal of first H atom gives $B_{12}H_{11}$, which has one electron in the dangling exohedral orbital. This can be used in the skeletal bonding. Removal of a second H atom brings in an additional electron to the skeletal bonding, so that $B_{12}H_{10}$ satisfies the Wade's rules. This is possible only if the bonding combination of the exohedral orbitals is not very low in energy in comparison to the higher lying skeletal bonding orbital. If the H atoms are removed from the adjacent positions, a situation similar to benzyne results.[56] The resulting bonding combination is not as stable as the exohedral orbitals are splayed out (Figure 2c,d). However, isomers, where H atoms are removed from nonadjacent positions, might be lower in energy due to better hyperconjugative stabilization of vacant dangling orbitals. Thus, 1,12- and 1,7-didehydrogeno $B_{12}H_{10}$ derivatives must have similar energy (Wade's rule satisfied), but lower than that of the 1,2-didehydrogeno $B_{12}H_{10}$ (Figure 2e,f).

Thus, structural preferences for B_nH_{n-2} and $B_nH_n^{2-}$ clusters should be similar since the removal of two H atoms adds the required electrons to the skeleton bonding. However, the effect of cluster size on diffuseness of exohedral orbitals and overlap between them determine the relative stability of the isomers in the polyhedral B_nH_{n-2} clusters. This is estimated by comparing the relative stability of neutral B_nH_{n-2} clusters for n = 6, 7, 10, and 12 to that of dianionic B_nH_{n-2} in Table 1. In smaller clusters, dangling orbitals on adjacent boron atoms are more splayed out (Figure 1) and would not have good overlap. In

DOI: 10.1021/acs.inorgchem.8b02986
Inorg. Chem. 2019, 58, 3627−3634

Table 1. Relative Energy (RE) in kcal/mol at CCSD(T)/6-311+G(d,p)//TPSSh/6-311+G(d,p) for Neutral and Dianionic B_nH_{n-2} Clusters with n = 6, 7, 10, and 12 (All Singlet State)[d]

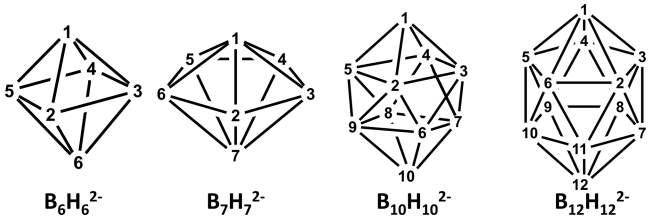

B_nH_{n-2}	RE for charge = 0	RE for charge = −2
1,2-B_6H_4	0.0[b]	22.0
1,6-B_6H_4	11.2	0.0
1,2-B_7H_5	4.5	32.8
2,3-B_7H_5	11.7[a]	4.1
2,4-B_7H_5	0.0	13.0[a]
1,7-B_7H_5	33.7	0.0
1,2-$B_{10}H_8$	26.7	0.8
2,3-$B_{10}H_8$	14.8	4.4
2,4-$B_{10}H_8$	2.5	7.4
2,6-$B_{10}H_8$	8.2	0.0
2,7-$B_{10}H_8$	0.0	13.6(10.8)[c]
1,6-$B_{10}H_8$	14.8	17.0(14.2)[c]
1,10-$B_{10}H_8$	31.0	6.5
1,2-$B_{12}H_{10}$	12.1	0.0
1,7-$B_{12}H_{10}$	0.0	14.7(13.4)[c]
1,12-$B_{12}H_{10}$	2.3	4.9

[a]Optimize to capped octahedron. [b]Most stable isomer for B_6H_4 is distorted pentagonal pyramid (see Figure S3, Supporting Information). [c]Triplet energies within parentheses. [d]The numbering scheme for isomers is given below. Optimized geometries of dianionic clusters are given in Figure S3 (Supporting Information).

order to enhance the overlap, structure distorts from ideal geometry. The excess two electrons, after satisfying n+1 SEPs in dianionic clusters, fill the lowest bonding combination of exohedral dangling orbitals and relative stability is reversed with respect to corresponding neutral clusters. The most stable isomer of $B_6H_4^{2-}$ corresponds to dehydrogenation at 1,6- and not 1,2-isomer. In contrast, 1,7- and 2,3-isomers are better for $B_7H_5^{2-}$. The structural deformations also destabilize cage isomers of B_6H_4 clusters (Table 1), and the semiplanar or the planar DC clusters are more stable. However, in larger clusters, dangling orbitals at adjacent boron atoms have slightly better overlap, since, as cluster size increases, the exohedral *sp* dangling orbitals would be less diffuse and less splayed out (Figure 1). This is also seen from the preference for larger polyhedra to fuse with smaller polyhedrons through a triangular face.[57] Thus, for $B_{10}H_8^{2-}$, dehydrogenation at 1,2-, 2,3-, and 2,6- are equally stabilizing, and for $B_{12}H_{10}^{2-}$, the most stable isomer corresponds to dehydrogenation at 1,2-position.

The energy difference of the bonding and antibonding combinations of the dangling orbitals of the dianionic B_nH_{n-2} isomers, with H atoms detached from adjacent positions, indicates the relative stability. The energy gap increases from 1.2 eV in 1,2-dehydro $B_6H_4^{2-}$ to 2.1 eV in 1,2-dehydro $B_{12}H_{10}^{2-}$ as shown in Figure 3. The better overlap for the exohedral dangling orbitals at the adjacent positions in the icosahedral $B_{12}H_{10}^{2-}$ cluster stabilizes the bonding combination to a slightly greater extent compared to the octahedral $B_6H_4^{2-}$ cluster. On the other hand, the antibonding

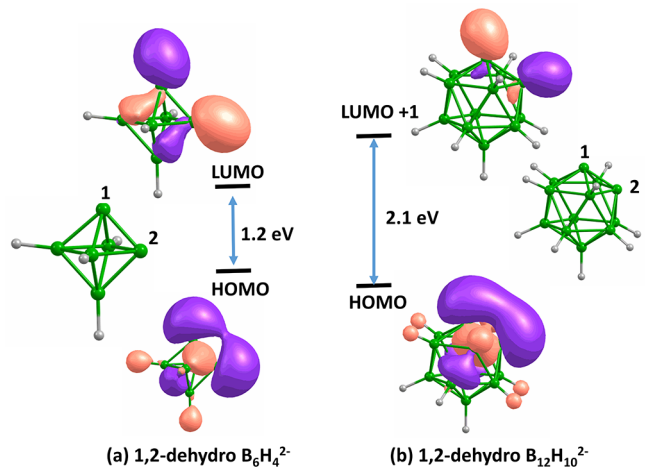

Figure 3. The separation between the bonding and antibonding combination of the exohedral dangling orbitals at adjacent positions for (a) 1,2-dehydro $B_6H_4^{2-}$ and (b) 1,2-dehydro $B_{12}H_{10}^{2-}$ clusters. The energy gap increases in (b) compared to (a), due to the better overlap of the dangling orbital combinations at adjacent boron atoms of the 1,2-dehydro $B_{12}H_{10}^{2-}$ clusters.

combination in 1,2-dehydro $B_{12}H_{10}^{2-}$ is destabilized to a greater extent and corresponds to LUMO+1, whereas, in 1,2-dehydro $B_6H_4^{2-}$, the LUMO corresponds to this combination. The energy difference between these two orbitals for the other dianionic B_nH_{n-2} clusters also increases as the size increases; however, due to lower symmetry, the orbitals would be more delocalized.

Further removal of H atoms from polyhedral clusters results in more electrons than required for skeletal bonding. For example, $B_{12}H_8$ attains the Wade's rule by taking two electrons from the four dangling bonds for skeletal bonding. This leaves two electrons in the bonding combination of the exohedral orbitals (Figure 2g). If the four H atoms are removed from adjacent positions, the bonding combination of a group of exohedral orbitals forms a delocalized stable MO, which is occupied by the two electrons. As more H atoms are removed, excess electrons from the dangling bonds occupy antibonding combinations of the dangling orbitals or skeletal antibonding orbitals. This would decrease the stability of the B-B skeleton and break the B−B bonds, gradually leading to flat structures. The reverse happens when H atoms are added to the planar cluster. Each new B−H bond removes an electron from the B−B bonding manifold of the cluster, ultimately leading to the n +1 skeletal electron pairs and polyhedral structures. This must be valid for smaller polyhedra as well. In the previous studies, the structural preferences for several of these borane clusters have been calculated by varying the H atoms using different methods.[19,20,23,58] We have recalculated the B_nH_x clusters with n varying from 5 to 12 and $x \leq n$ using similar density functional. The structural preferences are found to vary dramatically compared to previous reports in some clusters as pointed out in the following discussions. The B_nH_x isomers are denoted as ***n*c-*xy*** and ***n*p-*xy***, where ***n*** is the number of boron atoms, **c** and **p** represent the nature of the cluster as **c**age or **p**lanar, and ***x*** the number of H atoms. In addition, ***y*** takes alphabets **a**, **b**, **c**, etc., to represent structural isomers in decreasing stability order. Thus, **12c-8a** represents the $B_{12}H_8$ cage cluster, lowest in energy; **12c-8b** is the second-best cage cluster of $B_{12}H_8$. **12p-1a** and **12p-1b** denote the $B_{12}H$ planar structures, the latter being higher in energy.

DOI: 10.1021/acs.inorgchem.8b02986
Inorg. Chem. 2019, 58, 3627−3634

Structural Preferences of B_nH_xClusters with *n* Varying from 12 to 5 and $x \leq n$. The most stable isomers for the cage and planar $B_{12}H_x$ clusters are shown in Figures 4 and 5. The

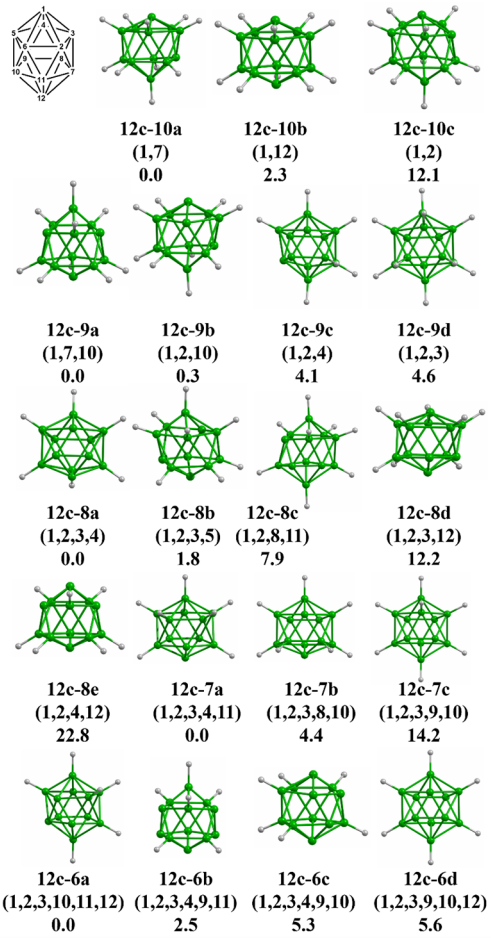

Figure 4. The most stable planar and the cage isomers of $B_{12}H_x$ clusters, with *x* from 10 to 6. The relative energy differences are given in kcal/mol at CCSD(T)/6-311+G(d,p)//TPSSh/6-311+G(d,p). The boron atom positions are indicated within parentheses, from where H atoms are detached.

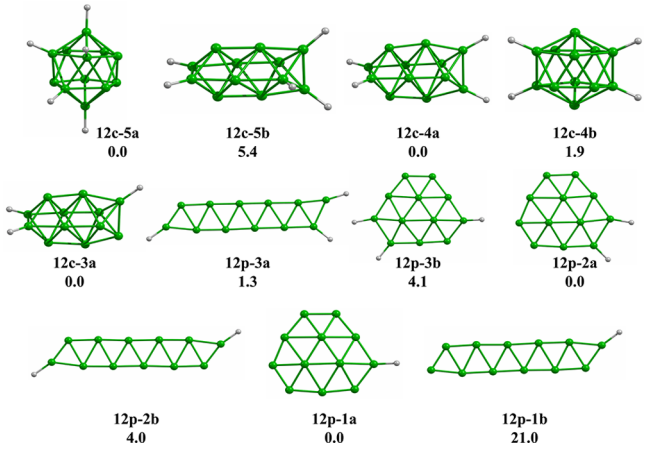

Figure 5. The most stable isomers of $B_{12}H_x$ clusters, with *x* from 5 to 1. The relative energy differences are given in kcal/mol, calculated at CCSD(T)/6-311+G(d,p)//TPSSh/6-311+G(d,p).

icosahedral type clusters for $B_{12}H_x$ are preferable up to the removal of six H atoms. The positions for the H atoms in the most stable icosahedral isomers from $B_{12}H_{10}$ to $B_{12}H_6$ clusters are denoted in Figure 4. $B_{12}H_{10}$ prefers both the H detached from boron atoms at meta (1,7-didehydro, **12c-10a**) and para (1,12-didehydro **12c-10b**) positions. The ortho isomer (1,2-didehydro, **12c-10c**) is less stable as anticipated. The $B_{12}H_9$ cluster has extra one electron to fill the bonding combination of dangling orbitals after required skeletal orbitals are occupied. The isomer with H atoms detached from the farthest boron atoms is equally stable as the one where H atoms are removed from adjacent two boron atoms. The lowest energy isomer of $B_{12}H_8$ (**12c-8a**) has H atoms removed from adjacent positions, such that excess electrons fill the in-phase combinations of the dangling orbitals. Removal of another H (addition of one electron to the system) did not change the icosahedral arrangement. All low energy structures remain icosahedral-like up to $B_{12}H_6$. But, as more number of H atoms are removed, such as with $x = 5$ and 4, alternate cage structures become equally stable or slightly more favorable compared to icosahedral isomers (Figure 5). While planar clusters of $B_{12}H_3$, **12p-3a**, and **12p-3b**, are almost degenerate in energy to a cage cluster **12c-3a**, planar isomers are global minimum (GM) geometries for $B_{12}H$ and $B_{12}H_2$ (**12p-1a** and **12p-2a**, respectively). This is in contrast to previous reports, where planar isomers are found to be GM up to $B_{12}H_3$.[23]

The reaction enthalpy for the consecutive removal of H atoms from $B_{12}H_x$ clusters as denoted by the reaction $B_{12}H_x \rightarrow B_{12}H_{x-1} + H$ is shown in Table T2 (Supporting Information). The heat of the reaction is endothermic in nature for all the clusters. Removal of H atom from $B_{12}H_{11}$, resulting in $B_{12}H_{10}$, has the lowest reaction enthalpy due to the satisfaction of the skeletal electron requirements. The removal of H atoms from the B_nH_x clusters become more endothermic as the number of H atoms decrease and is maximum for the formation of $B_{12}H$ from $B_{12}H_2$.

The smaller boron clusters (B_5 to B_{11}) show similar structural transformation upon variations in the attached H atoms. Table 2 summarizes the structural preferences of all the B_nH_x clusters. The detailed structural preferences of B_nH_x isomers for *n* varying from 11 to 5 are shown in the supplementary Figures S4–S10. The relative stability of the polyhedral B_nH_x clusters depends on the position of H atoms and the overlap of the exohedral dangling orbitals. The planar isomers are favorable up to B_nH_2 clusters. However, the

Table 2. Structural Preferences for B_nH_x Clusters Obtained after Energy Correction at CCSD/6-311+G(d,p)[c]

	structural preferences at *x* values		
B_nH_x	planar	degenerate	cage
B_5H_x	up to B_5H_3	B_5H_4	
B_6H_x	up to B_6H_3	B_6H_4	B_6H_5 onward
B_7H_x	up to B_7H_2		B_7H_3 onward
B_8H_x	up to B_8H_2	B_8H_3[a]	B_8H_4 onward
B_9H_x	up to B_9H_2	B_9H_3	B_9H_4 onward
$B_{10}H_x$	up to $B_{10}H_2$	$B_{10}H_3$	$B_{10}H_4$ onward
$B_{11}H_x$	up to $B_{11}H_2$	$B_{11}H_3$ and $B_{11}H_4$	$B_{11}H_5$ onward
$B_{12}H_x$	up to $B_{12}H_2$	$B_{12}H_3$[b]	$B_{12}H_4$ onward

[a] ΔE = 3.4 kcal/mol. [b] ΔE = 3.9 kcal/mol. [c] "degenerate" corresponds to energy differences between the most stable cage and planar isomers less than 2 kcal/mol, except for B_8H_3 and $B_{12}H_3$.

DOI: 10.1021/acs.inorgchem.8b02986
Inorg. Chem. 2019, 58, 3627–3634

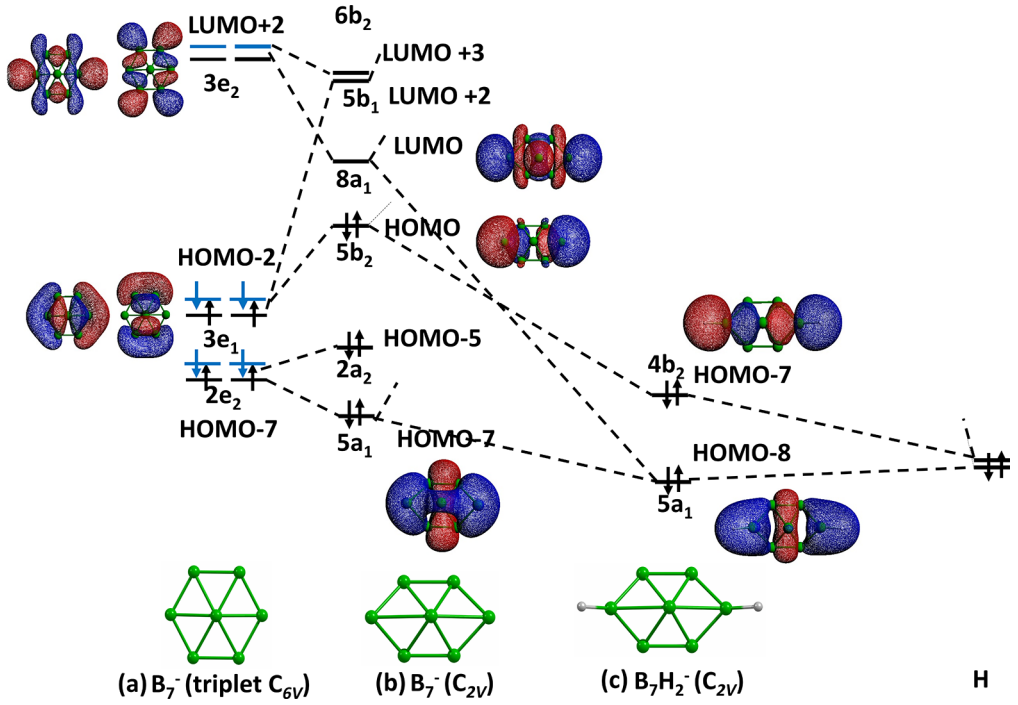

Figure 6. Orbital interaction diagram for disklike $B_7H_2^-$ cluster. The MOs involved in the bonding scheme are shown here.

hexagonal bipyramid is almost equally stable as planar isomers for B_8H (Figure S7). The relative stability of most favored cage and planar clusters is degenerate at B_nH_3. With four and more H atoms, polyhedral or alternate cage clusters are the most stable isomers. The polyhedral B_nH_x clusters become favorable with $x > n - 5$ for B_7H_x and B_8H_x; $x > n - 6$ for B_9H_x and $B_{10}H_x$; and $x > n - 7$ for $B_{11}H_x$ and $B_{12}H_x$ clusters. The B_5H_x and B_6H_x clusters show slight deviation. The clusters with an even number of electrons, as expected, are found to be stable with closed shell configurations, i.e., singlet spin state, whereas the clusters with an odd number of electrons have doublet as the ground state. The spin contamination for the unrestricted CCSD(T) energy corrections in open shell configurations is found to be very negligible, less than around 2%.

Orbital Interaction Diagram for Planar B_nH_2 Clusters. The planar DC geometries are more stable in the case of B_nH_2 clusters except for $B_{12}H_2$ and $B_{10}H_2$.[26−28] We have studied the orbital interactions involved, to understand their stability relative to disklike isomers as shown in Figures 6 and 7. The relevant orbitals involved in forming the BH bonds are only shown in these figures. The radial π orbitals of planar clusters participate to form BH bonds. These orbitals have greater coefficients at end boron atoms for the DC clusters,[28] whereas, in disklike clusters, in-plane "π" orbitals are delocalized throughout the peripheral ring.[59] The symmetric C_{6v} structure of disklike B_7^- is distorted to C_{2v} geometry after H addition as shown in Figure 6. Distortion in geometry reduces the symmetry of the frontier orbitals and increases the energy.

The DC clusters do not undergo any distortion in geometry to bind with H atoms. The in-plane π orbitals (HOMO and LUMO) and σ orbitals (HOMO-6 and HOMO-7) with greater coefficients at the peripheral boron atoms interact with the H atoms to form BH bond orbitals (Figure 7). The dangling orbitals on the other boron atoms have more overlap than would have been otherwise. The orbital interactions for DC B_n clusters with two H atoms enhance the stability for

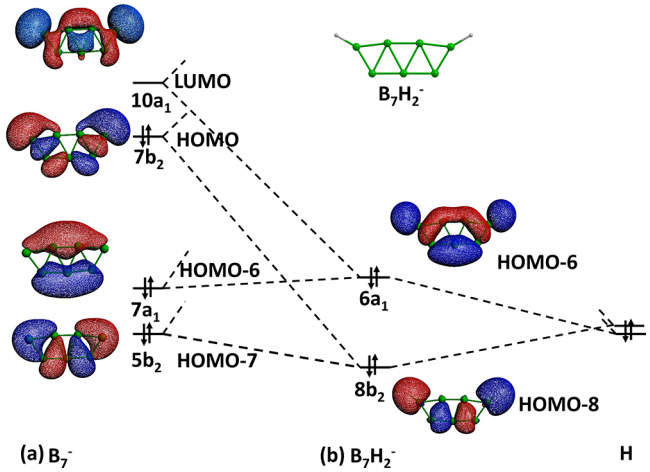

Figure 7. Orbital interaction diagram for double chain $B_7H_2^-$ cluster. The MOs involved in the bonding scheme are shown here.

most of the B_nH_2 clusters. With more H addition to DC clusters, some of the σ-skeletal orbitals participate in BH bond formation, and thus stability of DC isomers decreases and cage structures become more favorable, as seen earlier with B_6 and B_{20} clusters.[24,25]

Comparison of the Structural Preferences of Silico-Boron Clusters and B_nH_x Clusters. The structural information in B_nH_x clusters could be used to understand the preferences of silico-boron clusters. Si with a lone pair has an isolobal relationship with the BH unit.[60,61] Thus, B_nH and $B_{n-1}Si$ can be treated as isoelectronic. The most stable isomers for B_nSi clusters[31,32] with n varying from 4 to 11 are calculated at TPSSh/6-311+G(d,p). Structural preferences of B_nH and $B_{n-1}Si$ clusters are compared in Figure 8. The global minimum geometries for most $B_{n-1}Si$ clusters resemble the B_nH clusters. Slight variations are observed only for B_9Si and $B_{10}Si$ isomers. The $B_{n-2}Si_2$ should be isoelectronic to the B_nH_2 clusters. In

DOI: 10.1021/acs.inorgchem.8b02986
Inorg. Chem. 2019, 58, 3627−3634

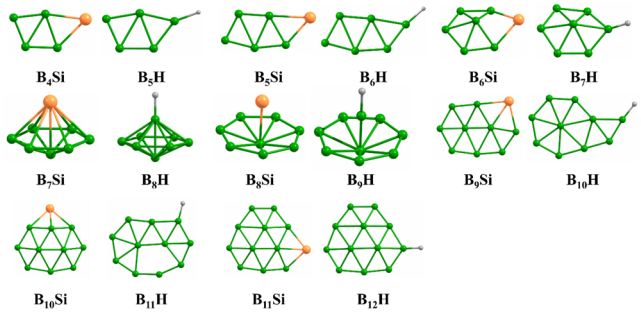

Figure 8. The structural similarity between the most stable isomers for $B_{n-1}Si$ and B_nH clusters, calculated at TPSSh/6-311+G(d,p). The relative stability of $B_{n-1}Si$ isomers is in good agreement with the previous reports (refs 31 and 32). Structural details for the most stable isomers of $B_{n-1}Si$ and B_nH clusters are given in the SI.

one of the recent reports, B_8Si_2 and $B_{10}Si_2$ clusters are found to be stable with DC structures and di-negative charges.[35] The silicon atoms occupy similar peripheral positions as BH units in the DC $B_{10}H_2^{2-}$ and $B_{12}H_2^{2-}$ clusters. The B_nSi_m clusters approach cage structures as the number of Si increases.[29,33,34,62] With $m > n$, the clusters would be equivalent of $B_n(BH)_m$ clusters, i.e., with a greater number of boron atoms attached with H atoms. Here, with an increase in number of Si atoms, more electrons are removed from skeletal orbitals to Si lone pair orbitals. Thus, similar to aromatic hydrocarbons, planar isomers become less stable and cage structures become favorable with an increase in the number of Si atoms. However, as the number of Si atoms increases, the cage structure of B_nSi_m clusters deviate from $B_n(BH)_m$ cage clusters due to variations in overlap interactions of bonding orbitals between silicon atoms in comparison to boron.[63,64]

CONCLUSIONS

The variation in geometry and electronic structures for B_nH_x clusters (n = 5−12, $x < n$) as a function of x is explained. Addition of H atoms removes electrons from skeletal orbitals. The reverse happens when H atoms are removed from $B_{12}H_{12}$, so that the icosahedral structure becomes flat. These structural transformations are similar to those observed for aromatic hydrocarbons where removal of electrons from benzene leads to pentagonal pyramidal and octahedral structures. The planar boron clusters remain stable up to the addition of 2−3 H atoms; beyond this, cage structures are favorable. However, structural distortions reduce the stability of B_6H_4 and B_5H_3 cage clusters. The structural preferences for silicon doped boron (Si_mB_n) clusters obey similar principles. As the number of Si atoms increases, cage structure is preferred. In this case, electrons are removed from skeletal orbitals to lone pair orbitals of Si, rendering the structural transformation. Thus, electronic structures and geometries of boron clusters could be tuned by doping suitably with Si atoms or attaching H atoms.

ASSOCIATED CONTENT

Supporting Information

The Supporting Information is available free of charge on the ACS Publications website at DOI: 10.1021/acs.inorgchem.8b02986.

Table T1 compares the relative stability of $B_{12}H_x$ clusters calculated at CCSD/6-311+G(d,p)//TPSSh/6-311+G(d,p), CCSD(T)/6-311+G(d,p)//TPSSh/6-311+G(d,p)b, and CCSD(T)/def2TZVP//B3LYP-D3/def2TZVP. Figures S1 and S2 give the corresponding structures of $B_{12}H_x$ isomers. Figure S3 shows the relative stability and structures of dianionic B_nH_{n-2} clusters for n corresponding to 6, 7, 10, and 12. Table T2 gives the reaction enthalpy for the consecutive removal of H atoms from $B_{12}H_x$ clusters. Figures S4−S10 show the most stable isomers of $B_{11}H_x$ to B_5H_x clusters, respectively. Table T3 gives the coordinates for the most stable isomers of $B_{n-1}Si$ and B_nH_x clusters (PDF)

AUTHOR INFORMATION

Corresponding Author

*E-mail: jemmis@iisc.ac.in.

ORCID

Eluvathingal D. Jemmis: 0000-0001-8235-3413

Notes

The authors declare no competing financial interest.

ACKNOWLEDGMENTS

We thank the Supercomputer Education and Research Centre, and Inorganic and Physical Chemistry Department, IISc, for computational facilities. N.K. thanks the Council of Scientific and Industrial Research for a Senior Research Fellowship, and R.C. thanks the Department of Science and Technology for the INSPIRE fellowship. E.D.J. acknowledges the Department of Science and Technology for the JC Bose fellowship.

REFERENCES

(1) Albert, B.; Hillebrecht, H. Boron: Elementary Challenge for Experimenters and Theoreticians. *Angew. Chem., Int. Ed.* **2009**, *48*, 8640−8668.

(2) Grimes, R. N. *Carboranes*; Academic Press: London, 2011.

(3) Jemmis, E.; Balakrishnarajan, M. The ubiquitous icosahedral B_{12} in boron chemistry. *Bull. Mater. Sci.* **1999**, *22*, 863−867.

(4) Karmodak, N.; Jemmis, E. D. Fragment approach to the electronic structure of τ-boron allotrope. *Phys. Rev. B: Condens. Matter Mater. Phys.* **2017**, *95*, 165128.

(5) Ogitsu, T.; Schwegler, E.; Galli, G. β-Rhombohedral Boron: At the Crossroads of the Chemistry of Boron and the Physics of Frustration. *Chem. Rev.* **2013**, *113*, 3425−3449.

(6) Boustani, I. New Convex and Spherical Structures of Bare Boron Clusters. *J. Solid State Chem.* **1997**, *133*, 182−189.

(7) Boustani, I. Systematic ab initio investigation of bare boron clusters: Determination of the geometry and electronic structures of B_n (n= 2−14). *Phys. Rev. B: Condens. Matter Mater. Phys.* **1997**, *55*, 16426.

(8) Niu, J.; Rao, B. K.; Jena, P. Atomic and electronic structures of neutral and charged boron and boron-rich clusters. *J. Chem. Phys.* **1997**, *107*, 132−140.

(9) Ricca, A.; Bauschlicher, C. W. The structure and stability of B_n^+ clusters. *Chem. Phys.* **1996**, *208*, 233−242.

(10) Sergeeva, A. P.; Popov, I. A.; Piazza, Z. A.; Li, W.-L.; Romanescu, C.; Wang, L.-S.; Boldyrev, A. I. Understanding Boron through Size-Selected Clusters: Structure, Chemical Bonding, and Fluxionality. *Acc. Chem. Res.* **2014**, *47*, 1349−1358.

(11) Huang, W.; Sergeeva, A. P.; Zhai, H.-J.; Averkiev, B. B.; Wang, L.-S.; Boldyrev, A. I. A concentric planar doubly π-aromatic B_{19}^- cluster. *Nat. Chem.* **2010**, *2*, 202−206.

(12) Li, W.-L.; Chen, X.; Jian, T.; Chen, T.-T.; Li, J.; Wang, L.-S. From planar boron clusters to borophenes and metalloborophenes. *Nat. Rev. Chem.* **2017**, *1*, 0071.

(13) Piazza, Z. A.; Hu, H. S.; Li, W. L.; Zhao, Y. F.; Li, J.; Wang, L. S. Planar hexagonal B_{36} as a potential basis for extended single-atom layer boron sheets. *Nat. Commun.* **2014**, *5*, 3113.

DOI: 10.1021/acs.inorgchem.8b02986
Inorg. Chem. 2019, 58, 3627−3634

(14) Sergeeva, A. P.; Piazza, Z. A.; Romanescu, C.; Li, W.-L.; Boldyrev, A. I.; Wang, L.-S. B_{22}^- and B_{23}^-: All-Boron Analogues of Anthracene and Phenanthrene. *J. Am. Chem. Soc.* **2012**, *134*, 18065−18073.
(15) Zhai, H.-J.; Kiran, B.; Li, J.; Wang, L.-S. Hydrocarbon analogues of boron clusters-planarity, aromaticity and antiaromaticity. *Nat. Mater.* **2003**, *2*, 827−833.
(16) Zhai, H.-J.; Zhao, Y.-F.; Li, W.-L.; Chen, Q.; Bai, H.; Hu, H.-S.; Piazza, Z. A.; Tian, W.- J.; Lu, H.-G.; Wu, Y.-B.; Mu, Y.-W.; Wei, G.-F.; Liu, Z.-P.; Li, J.; Li, S.-D.; Wang, L.-S. Observation of an all-boron fullerene. *Nat. Chem.* **2014**, *6*, 727−731.
(17) Zubarev, D. Y.; Boldyrev, A. I. Comprehensive analysis of chemical bonding in boron clusters. *J. Comput. Chem.* **2007**, *28*, 251−268.
(18) Zubarev, D. Y.; Boldyrev, A. I. Developing paradigms of chemical bonding: adaptive natural density partitioning. *Phys. Chem. Chem. Phys.* **2008**, *10*, 5207−5217.
(19) Ohishi, Y.; Kimura, K.; Yamaguchi, M.; Uchida, N.; Kanayama, T. Formation of hydrogenated boron clusters in an external quadrupole static attraction ion trap. *J. Chem. Phys.* **2008**, *128*, 124304.
(20) Ohishi, Y.; Kimura, K.; Yamaguchi, M.; Uchida, N.; Kanayama, T. Synthesis and formation mechanism of hydrogenated boron clusters $B_{12}H_n$ with controlled hydrogen content. *J. Chem. Phys.* **2010**, *133*, 074305.
(21) Fagiani, M. R.; Liu Zeonjuk, L.; Esser, T. K.; Gabel, D.; Heine, T.; Asmis, K. R.; Warneke. Opening of an icosahedral boron framework: A combined infrared spectroscopic and computational study. *Chem. Phys. Lett.* **2015**, *625*, 48−52.
(22) Farràs, P.; Vankova, N.; Zeonjuk, L. L.; Warneke, J.; Dülcks, T.; Heine, T.; Viñas, C.; Teixidor, F.; Gabel, D. From an Icosahedron to a Plane: Flattening Dodecaiodo-dodecaborate by Successive Stripping of Iodine. *Chem. - Eur. J.* **2012**, *18*, 13208−13212.
(23) Gonzalez Szwacki, N.; Tymczak, C. J. $B_{12}H_n$ and $B_{12}F_n$: Planar vs icosahedral structures. *Nanoscale Res. Lett.* **2012**, *7*, 236.
(24) Olson, J. K.; Boldyrev, A. I. Planar to 3D Transition in the B_6H_y Anions. *J. Phys. Chem. A* **2013**, *117*, 1614−1620.
(25) Bai, B.; Bai, H. Structural transition upon hydrogenation of B_{20} at different charge states: from tubular to disk-like, and to cage-like. *Phys. Chem. Chem. Phys.* **2016**, *18*, 6013−6020.
(26) Alexandrova, A. N.; Koyle, E.; Boldyrev, A. I. Theoretical study of hydrogenation of the doubly aromatic B_7^- cluster. *J. Mol. Model.* **2006**, *12*, 569−576.
(27) Li, D.-Z.; Chen, Q.; Wu, Y.-B.; Lu, H.-G.; Li, S.-D. Double-chain planar D_{2h} B_4H_2, C_{2h} B_8H_2, and C_{2h} $B_{12}H_2$: conjugated aromatic borenes. *Phys. Chem. Chem. Phys.* **2012**, *14*, 14769−14774.
(28) Li, W.-L.; Romanescu, C.; Jian, T.; Wang, L.-S. Elongation of planar boron clusters by hydrogenation: Boron analogues of polyenes. *J. Am. Chem. Soc.* **2012**, *134*, 13228−13231.
(29) Cao, G.-J.; Lu, S.-J.; Xu, H.-G.; Xu, X.-L.; Zheng, W.-J. Structures and electronic properties of $B_2Si_6^{-/0/+}$: anion photoelectron spectroscopy and theoretical calculations. *RSC Adv.* **2016**, *6*, 62165−62171.
(30) Li, W.-L.; Romanescu, C.; Galeev, T. R.; Wang, L.-S.; Boldyrev, A. I. Aluminum Avoids the Central Position in AlB_9^- and AlB_{10}^-: Photoelectron Spectroscopy and ab Initio Study. *J. Phys. Chem. A* **2011**, *115*, 10391−10397.
(31) Mai, D. T. T.; Duong, L. V.; Tai, T. B.; Nguyen, M. T. Electronic Structure and Thermochemical Parameters of the Silicon-Doped Boron Clusters B_nSi, with n = 8−14, and Their Anions. *J. Phys. Chem. A* **2016**, *120*, 3623−3633.
(32) Tai, T. B.; Kadłubański, P.; Roszak, S.; Majumdar, D.; Leszczynski, J.; Nguyen, M. T. Electronic Structures and Thermochemical Properties of the Small Silicon-Doped Boron Clusters B_nSi (n=1−7) and Their Anions. *ChemPhysChem* **2011**, *12*, 2948−2958.
(33) Tam, N. M.; Tai, T. B.; Nguyen, M. T. Thermochemical Parameters and Growth Mechanism of the Boron-Doped Silicon Clusters, Si_nB^q with n = 1−10 and q = −1, 0, +1. *J. Phys. Chem. C* **2012**, *116*, 20086−20098.
(34) Truong, N. X.; Jaeger, B. K. A.; Gewinner, S.; Schöllkopf, W.; Fielicke, A.; Dopfer, O. Infrared Spectroscopy and Structures of Boron-Doped Silicon Clusters (Si_nB_m, n = 3−8, m = 1−2). *J. Phys. Chem. C* **2017**, *121*, 9560−9571.
(35) Van Duong, L.; Tho Nguyen, M. Silicon doped boron clusters: how to make stable ribbons? *Phys. Chem. Chem. Phys.* **2017**, *19*, 14913−14918.
(36) Giordano, C.; Heldeweg, R. F.; Hogeveen, H. Pyramidal dications. Introduction of basal and apical substituents. *J. Am. Chem. Soc.* **1977**, *99*, 5181−5183.
(37) Hogeveen, H.; Kwant, P. Chemistry and spectroscopy in strongly acidic solutions. XL. $(CCH_3)_6^{2+}$, an unusual dication. *J. Am. Chem. Soc.* **1974**, *96*, 2208−2214.
(38) Jemmis, E. D.; Jayasree, E. G.; Parameswaran, P. Hypercarbons in polyhedral structures. *Chem. Soc. Rev.* **2006**, *35*, 157−168.
(39) Jemmis, E. D.; Schleyer, P. v. R. Aromaticity in three dimensions. 4. Influence of orbital compatibility on the geometry and stability of capped annulene rings with six interstitial electrons. *J. Am. Chem. Soc.* **1982**, *104*, 4781−4788.
(40) Malischewski, M.; Seppelt, K. Crystal Structure Determination of the Pentagonal-Pyramidal Hexamethyl benzene Dication $C_6(CH_3)_6^{2+}$. *Angew. Chem., Int. Ed.* **2017**, *56*, 368−370.
(41) Pham, H. T.; Duong, L. V.; Pham, B. Q.; Nguyen, M. T. The 2D-to-3D geometry hopping in small boron clusters: The charge effect. *Chem. Phys. Lett.* **2013**, *577*, 32−37.
(42) Kiran, B.; Bulusu, S.; Zhai, H.-J.; Yoo, S.; Zeng, X. C.; Wang, L.-S. Planar-to-tubular structural transition in boron clusters: B_{20} as the embryo of single-walled boron nanotubes. *Proc. Natl. Acad. Sci. U. S. A.* **2005**, *102*, 961−964.
(43) Arvanitidis, A. G.; Lim, K. Z.; Havenith, R. W. A.; Ceulemans, A. Valence bonds in elongated boron clusters. *Int. J. Quantum Chem.* **2018**, *118*, No. e25575.
(44) Frisch, M. J.; Trucks, G. W.; Schlegel, H. B.; Scuseria, G. E.; Robb, M. A.; Cheeseman, J. R.; Scalmani, G.; Barone, V.; Mennucci, B.; Petersson, G. A.; Nakatsuji, H.; Caricato, M.; Li, X.; Hratchian, H. P.; Izmaylov, A. F.; Bloino, J.; Zheng, G.; Sonnenberg, J. L.; Hada, M.; Ehara, M.; Toyota, K.; Fukuda, R.; Hasegawa, J.; Ishida, M.; Nakajima, T.; Honda, Y.; Kitao, O.; Nakai, H.; Vreven, T.; Montgomery, J. A., Jr.; Peralta, J. E.; Ogliaro, F.; Bearpark, M.; Heyd, J. J.; Brothers, E.; Kudin, K. N.; Staroverov, V. N.; Kobayashi, R.; Normand, J.; Raghavachari, K.; Rendell, A.; Burant, J. C.; Iyengar, S. S.; Tomasi, J.; Cossi, M.; Rega, N.; Millam, J. M.; Klene, M.; Knox, J. E.; Cross, J. B.; Bakken, V.; Adamo, C.; Jaramillo, J.; Gomperts, R.; Stratmann, R. E.; Yazyev, O.; Austin, A. J.; Cammi, R.; Pomelli, C.; Ochterski, J. W.; Martin, R. L.; Morokuma, K.; Zakrzewski, V. G.; Voth, G. A.; Salvador, P.; Dannenberg, J. J.; Dapprich, S.; Daniels, A. D.; Farkas, Ö.; Foresman, J. B.; Ortiz, J. V.; Cioslowski, J.; Fox, D. J. *Gaussian 09*, Revision D.01; Gaussian, Inc.: Wallingford, CT, 2009.
(45) Perdew, J. P.; Kurth, S.; Zupan, A.; Blaha, P. Accurate Density Functional with Correct Formal Properties: A Step Beyond the Generalized Gradient Approximation. *Phys. Rev. Lett.* **1999**, *82*, 2544−2547.
(46) Perdew, J. P.; Tao, J.; Staroverov, V. N.; Scuseria, G. E. Meta-generalized gradient approximation: Explanation of a realistic nonempirical density functional. *J. Chem. Phys.* **2004**, *120*, 6898−6911.
(47) Tao, J.; Perdew, J. P.; Staroverov, V. N.; Scuseria, G. E. Climbing the Density Functional Ladder: Nonempirical Meta-Generalized Gradient Approximation Designed for Molecules and Solids. *Phys. Rev. Lett.* **2003**, *91*, 146401.
(48) Clark, T.; Chandrasekhar, J.; Spitznagel, G. W.; Schleyer, P. V. R. Efficient diffuse function-augmented basis sets for anion calculations. III. The 3-21+G basis set for first-row elements, Li−F. *J. Comput. Chem.* **1983**, *4*, 294−301.
(49) Krishnan, R.; Binkley, J. S.; Seeger, R.; Pople, J. A. Self-consistent molecular orbital methods. XX. A basis set for correlated wave functions. *J. Chem. Phys.* **1980**, *72*, 650−654.

DOI: 10.1021/acs.inorgchem.8b02986
Inorg. Chem. 2019, 58, 3627−3634

(50) McLean, A. D.; Chandler, G. S. Contracted Gaussian basis sets for molecular calculations. I. Second row atoms, Z=11−18. *J. Chem. Phys.* **1980**, *72*, 5639−5648.
(51) Li, F.; Jin, P.; Jiang, D.-e.; Wang, L.; Zhang, S. B.; Zhao, J.; Chen, Z. B_{80} and $B_{101-103}$ clusters: Remarkable stability of the core-shell structures established by validated density functionals. *J. Chem. Phys.* **2012**, *136*, 074302.
(52) Čížek, J. On the use of the cluster expansion and the technique of diagrams in calculations of correlation effects in atoms and molecules. *Adv. Chem. Phys.* **2007**, 35−89.
(53) Knowles, P. J.; Hampel, C.; Werner, H. J. Coupled cluster theory for high spin, open shell reference wave functions. *J. Chem. Phys.* **1993**, *99*, 5219−5227.
(54) Raghavachari, K.; Trucks, G. W.; Pople, J. A.; Head-Gordon, M. A fifth-order perturbation comparison of electron correlation theories. *Chem. Phys. Lett.* **1989**, *157*, 479−483.
(55) te Velde, G.; Bickelhaupt, F. M.; Baerends, E. J.; Fonseca Guerra, C.; van Gisbergen, S. J. A.; Snijders, J. G.; Ziegler, T. Chemistry with ADF. *J. Comput. Chem.* **2001**, *22*, 931−967.
(56) Pancharatna, P. D.; Balakrishnarajan, M. M.; Jemmis, E. D.; Hoffmann, R. Polyhedral Borane Analogues of the Benzynes and Beyond: Bonding in Variously Charged $B_{12}H_{10}$ Isomers. *J. Am. Chem. Soc.* **2012**, *134*, 5916−5920.
(57) Shameema, O.; Jemmis, E. D. Orbital Compatibility in the Condensation of Polyhedral Boranes. *Angew. Chem., Int. Ed.* **2008**, *47*, 5561−5564.
(58) Böyükata, M.; Özdoğan, C.; Güvenç, Z. B. Effects of hydrogen hosting on cage structures of boron clusters: density functional study of B_mH_n (m = 5−10 and n ≤ m) complexes. *Phys. Scr.* **2008**, *77*, 025602.
(59) Alexandrova, A. N.; Boldyrev, A. I.; Zhai, H.-J.; Wang, L.-S. Electronic Structure, Isomerism, and Chemical Bonding in B_7^- and B_7. *J. Phys. Chem. A* **2004**, *108*, 3509−3517.
(60) Hoffmann, R. Building Bridges Between Inorganic and Organic Chemistry (Nobel Lecture). *Angew. Chem., Int. Ed. Engl.* **1982**, *21*, 711−724.
(61) Jemmis, E. D.; Srinivas, G. N. Contrasting Stabilities of Classical and Bridged Pyramidal Si_3H_3X Molecules (X = BH-, CH, N, NH+, NO, SiH, P, PH+, and PO). *J. Am. Chem. Soc.* **1996**, *118*, 3738−3742.
(62) Lu, S.-J.; Xu, X.-L.; Cao, G.-J.; Xu, H.-G.; Zheng, W.-J. Structural Evolution of $B_2Si_n^{-/0}$ (n = 3−12) Clusters: Size-Selected Anion Photoelectron Spectroscopy and Theoretical Calculations. *J. Phys. Chem. C* **2018**, *122*, 2391−2401.
(63) Jemmis, E. D.; Subramanian, G.; Radom, L. closo-Silaboranes and closo-carboranes: contrasting relative stabilities and breakdown of the rule of topological charge stabilization. *J. Am. Chem. Soc.* **1992**, *114*, 1481−1483.
(64) Kiran, B.; Anoop, A.; Jemmis, E. D. Control of Stability through Overlap Matching: closo-Carborynes and closo-Silaborynes. *J. Am. Chem. Soc.* **2002**, *124*, 4402−4407.

DOI: 10.1021/acs.inorgchem.8b02986
Inorg. Chem. 2019, 58, 3627−3634